SANDIA REPORT

SAND2013-8278
Unlimited Release
Printed September 2013

Predictive Modeling of Reactive Wetting and Metal Joining

Frank B. van Swol

Prepared by
Sandia National Laboratories
Albuquerque, New Mexico 87185 and Livermore, California 94550

Sandia National Laboratories is a multi-program laboratory managed and operated by Sandia Corporation, a wholly owned subsidiary of Lockheed Martin Corporation, for the U.S. Department of Energy's National Nuclear Security Administration under contract DE-AC04-94AL85000.

Approved for public release; further dissemination unlimited.

Sandia National Laboratories

Issued by Sandia National Laboratories, operated for the United States Department of Energy by Sandia Corporation.

NOTICE: This report was prepared as an account of work sponsored by an agency of the United States Government. Neither the United States Government, nor any agency thereof, nor any of their employees, nor any of their contractors, subcontractors, or their employees, make any warranty, express or implied, or assume any legal liability or responsibility for the accuracy, completeness, or usefulness of any information, apparatus, product, or process disclosed, or represent that its use would not infringe privately owned rights. Reference herein to any specific commercial product, process, or service by trade name, trademark, manufacturer, or otherwise, does not necessarily constitute or imply its endorsement, recommendation, or favoring by the United States Government, any agency thereof, or any of their contractors or subcontractors. The views and opinions expressed herein do not necessarily state or reflect those of the United States Government, any agency thereof, or any of their contractors.

Printed in the United States of America. This report has been reproduced directly from the best available copy.

Available to DOE and DOE contractors from
U.S. Department of Energy
Office of Scientific and Technical Information
P.O. Box 62
Oak Ridge, TN 37831

Telephone: (865) 576-8401
Facsimile: (865) 576-5728
E-Mail: reports@adonis.osti.gov
Online ordering: http://www.osti.gov/bridge

Available to the public from
U.S. Department of Commerce
National Technical Information Service
5285 Port Royal Rd
Springfield, VA 22161

Telephone: (800) 553-6847
Facsimile: (703) 605-6900
E-Mail: orders@ntis.fedworld.gov
Online ordering: http://www.ntis.gov/help/ordermethods.asp?loc=7-4-0#online

SAND2013-8278
Unlimited Release
Printed September 2013

Predictive Modeling of Reactive Wetting and Metal Joining

Frank B. van Swol
Department 1814
Sandia National Laboratories
Albuquerque, NM 87185-1411
fbvansw@sandia.gov

Abstract

The performance, reproducibility and reliability of metal joints are complex functions of the detailed history of physical processes involved in their creation. Prediction and control of these processes constitutes an intrinsically challenging multi-physics problem involving heating and melting a metal alloy and reactive wetting. Understanding this process requires coupling strong molecular-scale chemistry at the interface with microscopic (diffusion) and macroscopic mass transport (flow) inside the liquid followed by subsequent cooling and solidification of the new metal mixture. The final joint displays compositional heterogeneity and its resulting microstructure largely determines the success or failure of the entire component. At present there exists no computational tool at Sandia that can predict the formation and success of a braze joint, as current capabilities lack the ability to capture surface/interface reactions and their effect on interface properties. This situation precludes us from implementing a proactive strategy to deal with joining problems. Here, we describe what is needed to arrive at a predictive modeling and simulation capability for multi-component metals with complicated phase diagrams for melting and solidification, incorporating dissolutive and composition-dependent wetting.

Acknowledgment

Thanks to Carlton Brooks, Scott Roberts, Rick Givler, Mike Chandross, Jeremy Lechman and Allen Roach for stimulating discussions of reactive wetting, level set methods, goniometers and active brazing.

Contents

Preface **9**

Summary **11**

1 Introduction **13**

2 Interfacial Phenomena **15**

Problem statement 15

Diffuse interfaces 18

Temperature gradients 18

Solidification 18

3 Moving Contact Lines **21**

The moving contact line on a solid surface 21

Blake's approach [9, 10] 21

Shikhmurzaev's approach [8, 10] 22

Moving contact line for reactive wetting 24

4 Surface Tensions **27**

Modeling liquid metal mixtures 27

Equilibrium and nonequilibrium surface tensions 28

Validation experiments 30

5 Conclusion **35**

References **36**

List of Figures

1.1 Schematic of the simplest reactive wetting problems of interest: a liquid metal droplet spreading on a solid surface (on the left, (a)) and a metal fluid infiltrating a channel (on the right, (b)). In both cases surface reactions (e.g., dissolution from the solid phase, or deposition from the fluid phase) are present. The simplest reaction, an isomerization reaction, where molecules A are converted into molecules B serves as a general example. While spreading and infiltration take place the composition changes inside the fluid, starting at the liquid-solid interface. The surface reaction changes the composition throughout the liquid, and is generally expected to be strongly nonuniform. Note, that the consequence of a surface reaction can also be reduced wetting. The general challenge to be addressed is to predict the final shape and composition distribution. 14

2.1 Diagram of the proposed predictive computational fluid dynamics (CFD) model for reactive wetting. The CFD requires diffusion parameters (i) for mass transport, and viscosity information (j) to solve the Navier-Stokes equations. The boundary conditions (BC) needed for the contact line movement are one of two approaches, one suggested by Blake the other by Shikhmurzaev. Both require adaptation to nonuniform mixtures and interfacial tension information(k). The mutual diffusion coefficients for metal mixtures can be obtained (a), ultimately, from self-diffusion coefficients that are either generated by molecular dynamics (MD) or molecular kinetic theory (e.g., Enskog approximations). The viscosity can be obtained (b) from MD or molecular theory. The interfacial tensions (k) that feed into the contact angle BCs can be obtained from the noneqilibrium density profiles (c&d). This can be accomplished by MD or classical fluids DFT. Alternatively, the nonequilibrium profiles produce nonequilibrium tensions by developing methods that use equilibrium information. That is indicated by the path (h, f, g). The required equilibrium tensions can be generated by MD or DFT (see path(e,f)). The color scheme for the boxes is as follows. Black indicates that the methods or data are well-established. Green indicates that established simulation of theoretical methods need to be used to generate the information. Red indicates that some level of new science and innovative research is required. The strategy to accomplish that is described in this document. 17

3.1 Shematic of the contact line. Young's equation is illustrated on the left. On the right hand side we illustrate the flow (ala Shikhmurzaev) in the vicinity of the contact line. The interfaces are depicted as layers of finite thickness so that the velocity distribution across the interface can be depicted. The extent of the contact line region (II) is of the order of Ca (the capillary number). Note that at the solid boundary, and away from the contact line, the magnitude of v^s increases. Slip is present only in the contact region. 23

4.1 The equilibrium surface tension of a solid-liquid interface, Ω_{wl}/A (green curve) for a binary fluid of overall composition x_B. 28

4.2 A surface reaction-diffusion process. At the left-hand side wall the reaction is $A(red) \rightarrow B(gray)$. To enhance the visibility of species B(gray), the size of atoms A have been reduced. Snapshots taken at different times, progressing from top to bottom. The right-hand side of the box contains a vapor phase. This is a convenient and simple way to represent a *constant* low vapor pressure. 29

4.3 A surface reaction-diffusion process. Density profiles $\rho_A(z)$ (blue curves) and $\rho_B(z)$ (red curves) at different times t. Note the transient, non-equilibrium nature of the profiles; all product profiles (i.e., $\rho_B(z)$) approach zero, at larger distances. We can associate a thickness $\mathscr{L}$ with each nonequilibrium profile. 31

4.4 A simulation example of the development of the surface tension (here denoted as the surface grand potential per unit area, Ω_s/A) as a function of time, for a surface reaction $A \rightarrow B$. Two cases are shown, differing in the value for the surface reaction probability ($p_r = 0.005$ and $p_r = 0.001$). An estimated surface free energy is shown as a black line. It is based on an integral of the transient profiles shown in figure 4.3. 32

4.5 Schematic of a feed-through goniometer. This set-up allows the contact-angle measurement of a static sessile drop, or that of a dynamic contact angle at various velocities. see Brooks et al.[30] 33

Preface

When a liquid droplet is placed on a surface in the presence of gravity, we find that its final shape, and hence the amount of liquid that is in contact with the solid, is solely function of the contact angle. For droplets that are not too small (e.g., nanodroplets) the contact angle is a geometric quantity that can be readily measured in the laboratory. For all sizes, it is also a thermodynamic quantity, as was first pointed out by Thomas Young in the early 1800's. Young showed that the cosine of the contact angle equals a dimensionless ratio of the difference in surface free energies (”surface tensions”) between the solid-liquid and the solid-vapor interfaces,and the liquid-vapor tension. It is a sobering thought that the entire shape of a macroscopic droplet is determined entirely by the asymmetry in forces acting in the interfacial regions, which have a thickness of the order of a nanometer. Thus a tiny fraction of the liquid, negligible by volume, governs the entire droplet shape. Similar observations apply to other interfacial phenomena, such as capillary rise.

The surface tensions, and therefore the contact angle, can be sensitive to variations in composition. Indeed, trace amounts (by volume) of surface active molecules can drastically change the tensions. For that same reason, the presence of impurities can (but do not have to) have significant consequences for the surface tensions. It follows that the compositional changes have to be manifest at the interface(s) to lead to contact angle changes.

A special case of (potentially rapid) compositional change is presented by surface-reactive systems. These are systems where the local composition changes at one of the interfaces due dissolution, absorption, adsorption, or due to a surface chemical reaction. In this report, the general wetting and spreading behavior of such systems is collectively referred to as ”reactive wetting”. In practice this is sometimes a desired effect. An example of this is active brazing, where a small amount of Zr is added to a Ag based braze for applications involving the joining of metals with alumina parts. The Zr replaces Al atoms in alumina and that process improves the wetting behavior of the braze.

Predictive continuum-level simulations of capillary flow are applied in a wide range of applications, ranging from mold filling (e.g., encapsulation) to transport in geological formations (e.g., CO_2 sequestration). However, none of the current simulation techniques can handle reactive wetting. This report addresses the reasons for this lack of capabilities and identifies a coherent approach that links molecular scale phenomena, such as surface reactions, to macroscopic phenomena such as capillary-driven flow. We refer the interested reader to a companion report (SAND2013-8155, see reference[49]) for some additional details regarding the equilibrium behavior of metals and metal alloys.

This page intentionally left blank.

Summary

Dynamic wetting of liquids is a process that operates on multiple length scales stretching from the molecular scale (e.g., contact line, surface reaction) to the macroscopic (the entire metal joint). Capturing the physics of molecular scale effects that are known to manifest at the macroscopic scale is the big challenge we address in this report. We propose a novel coherent framework for predictive modeling of metal joining, identifying the various pieces that must be addressed and strategy to accomplish this. In particular, we will outline a multi-component modeling capability that resolves spatial inhomogeneities and transients, by generating crucial interfacial properties (i.e., tensions) from molecular scale interactions. Other approaches have not spatially resolved multi-component transport nor accounted for interfacial phenomena (e.g., wetting and spreading).

In this report we introduce the first multi-physics model to simulate dynamic wetting and free surface flow for a reacting multi-component liquid. The unique aspects of this model are a spatially resolved composition and its consequences on the interfacial tensions. Understanding the interfacial flow profile is of critical importance in a host of processes, including metal joining, metal relocation, inkjet printing, additive manufacturing and flow through porous rock. This is because the composition of a multi- component fluid near the interface can strongly affect interfacial properties such as surface tension and contact angles. The basic challenge is to understand these behaviors and capture them in a continuum-level computation model. Such a model can be implemented in existing continuum codes (cf., Sierra/Aria) and used to study dynamic wetting issues that plague current processes around the weapons complex such as metal joining and Al relocation, as well as in areas of national interest such as CO_2 sequestration.

This page intentionally left blank.

Chapter 1

Introduction

In this paper we discuss the phenomenon of metal joining. In particular, we consider creating a metal bond by contacting a liquid metal (pure or alloy) with a rigid metal surface. This is a situation that is commonly encountered during (laser) welding, brazing and thermal spraying. The liquid metal will spread onto the rigid surface, or infiltrate a narrow gap, while possibly changing composition due to surface processes (”surface reactions”). This dynamic process will be coupled to or followed by cooling and in all cases eventually result in solidification. The ultimate goal is to provide a continuum level predictive modeling capability that will faithfully describe this entire process, and will be able to provide information and insight about the final microstructure of the resulting bond.

Dynamic wetting by liquid is a process that operates on multiple length scales stretching from the molecular scale (e.g., contact line, surface reaction) to the macroscopic (the entire metal joint). Usually, experimental information covers just the macroscopic scale. That is, the wetting speed, contact angle, and viscosity are usually measured over length scales that are greater than microns. Yet, as is well-known, surface tensions can be greatly influenced by processes such as adsorption, that take place on the molecular scale, while affecting the macroscopic scale[1]. Thus, it is clear that the task of developing a predictive modeling approach is a difficult one. In this paper we will present a framework for predictive modeling of metal joining, and identify the various pieces that need to be addressed in order to accomplish this. Then we will outline, in detail, an approach that is firmly based in thermodynamics and statistical mechanics, that can provide the required thermodynamic and dynamic information.

[1] An illustrative example is provided by the Washburn equation that says that the infiltration distance is proportional to the square root of time, with a proportionality constant that is equal to the square root of the difference in the solid-vapor and solid-liquid surface tensions. The latter is highly sensitive to the surface reactions and dissolution. Thus the infiltration speed will be a sensitive function of the reactive phenomena at the solid liquid boundary.

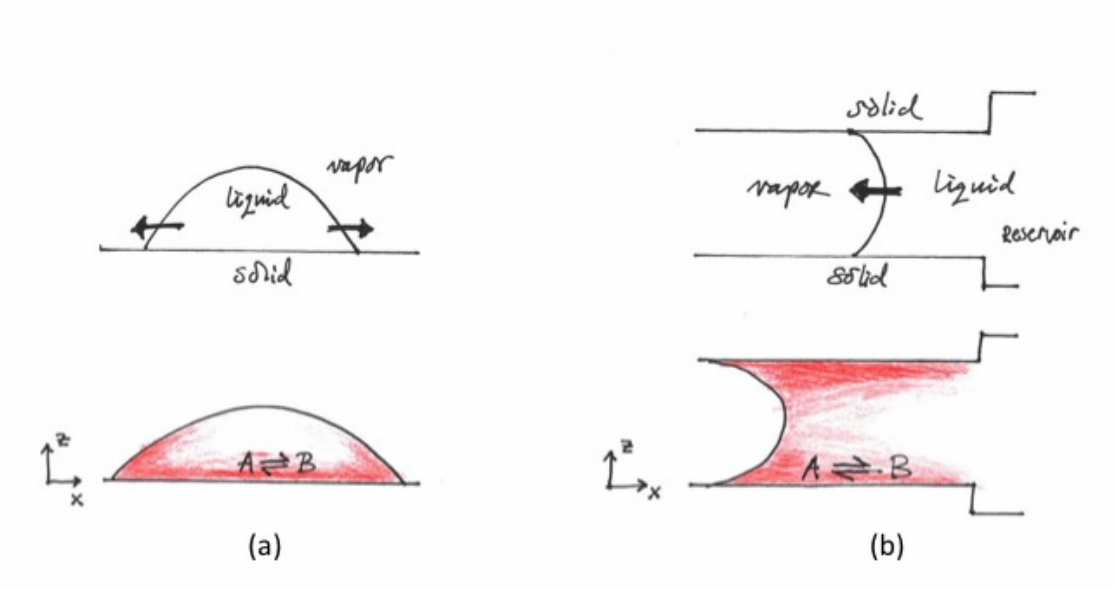

Figure 1.1. Schematic of the simplest reactive wetting problems of interest: a liquid metal droplet spreading on a solid surface (on the left, (a)) and a metal fluid infiltrating a channel (on the right, (b)). In both cases surface reactions (e.g., dissolution from the solid phase, or deposition from the fluid phase) are present. The simplest reaction, an isomerization reaction, where molecules A are converted into molecules B serves as a general example. While spreading and infiltration take place the composition changes inside the fluid, starting at the liquid-solid interface. The surface reaction changes the composition throughout the liquid, and is generally expected to be strongly nonuniform. Note, that the consequence of a surface reaction can also be reduced wetting. The general challenge to be addressed is to predict the final shape and composition distribution.

Chapter 2

Interfacial Phenomena

Problem statement

Continuum-level modeling of a moving fluid-solid interfacial boundary can be accomplished with finite element codes such as Sandia's GOMA and ARIA. Such modeling requires the ability to handle Newtonian flow and, specifically, a dynamical treatment of the three-phase contact line. It is well-known that within continuum dynamics the contact line represents a line (or point) of divergence of the fluid stress. This presents a significant technical problem that has, however, been successfully addressed in the past. Two approaches have become well-accepted. Blake [9, 10] has put forth a method, based on molecular kinetics ideas, that allows for the movement of the contact line. This approach is currently part of both GOMA and ARIA [11], but for fluids that are of *uniform* composition only. As an alternative, Shikhmurzaev [8, 10] has developed a more radical approach based on hydrodynamics of the surface layer, explicitly modeling the interfacial transformation process taking place at the wetting line. This technique is not currently available in either GOMA or ARIA.

A liquid metal spreading on a metal surface introduces additional complexities into the description of the moving fluid-solid interfacial boundary. Primary amongst these are the effects of mixing, preferential adsorption and dissolution processes that are common at the solid-fluid interface. That is, metal atoms of the rigid solid may leave the solid and dissolve into the liquid metal. Simultaneously, metal atoms in the liquid may leave the liquid and be integrated into the solid boundary. These two mixing processes will affect the local composition of the liquid as well as the solid. In adsorption processes, inhomogeneous composition throughout the interface may develop as one species of the liquid exhibits preferential adsorption at the solid-liquid interface.

No matter what the underlying causes, composition changes of the liquid and solid phases will produce a change in the liquid-solid interfacial free energy ("surface tension"[1]) as well as possibly in the transport properties (i.e., the viscosity). Changes in the surface tension imply a variation in the contact angle, which will influence the movement of the contact line. Thus, formally, the contact angle, θ, is to be considered a function of the interfacial composition, which itself is a function of time. The variable contact angle serves as input to the continuum modeling if we

[1] Strictly, a surface free energy per unit area. For liquid-vapor interfaces the surface free energy is always positive, thus justifying the term "tension". However, at a solid boundary the surface free energy can be of either sign. In practice, the sign does not affect the convention to use the term surface tension for all interfaces.

employ Blake's approach [9, 10] to describe the moving contact line. Under Shikhmurzaev's scheme [8, 10] the surface tension of the interfaces changes on account of the local *surface density* and composition (combined with a surface equation of state).

To make progress, the top-down strategy outlined here implies that we have (or develop) a means to predict the value of the contact angle as the dissolution proceeds. This constitutes a challenging problem. The dissolution (into the liquid phase) and deposition (into the solid phase) is obviously a non-equilibrium, non-steady state process. It clearly must depend on (at least) the solubility of the various components in both phases, the rate of dissolution, the free energy change upon dissolution (or deposition), and the rate of diffusion. In addition, we recognize that, in general, there may also be thermal gradients (e.g., a hot metal spreading on a cold substrate) present, and phase changes (e.g., solidification) taking place in the interfacial region that modify the geometry of the solid-liquid boundary from perfectly planar and smooth to a rough boundary.

This paper seeks to outline a systematic procedure (see the scheme depicted in figure 2.1), firmly based in statistical mechanics, for predicting the changes in the interfacial composition and calculating its consequences for the contact angle. The interfacial composition of any interface is fully defined by the density profiles of each of the M, say, component, i.e., $\rho_k(\mathbf{r},t)$; $k = 1,M$, a function of position and time; and from this we seek to predict the surface free energy, $\Omega^s(t)$ of that interface as a function of time. We will initially do so for a system that is not the most general, but sufficiently rich to be of relevance to the problem at hand.

In the sections that follow we will address each of the "boxes" and connectors shown in figure 2.1, which constructs a path from molecular interactions and molecular considerations to the macroscopic length scale of computational fluid dynamics (CFD). As we will see, metal liquid mixtures are relatively simple, thanks to the atomic nature of metals. As a consequence, it is relatively straightforward to produce accurate thermodynamic and diffusion data needed as input by the CFD. We will show that the primary scientific challenges are:

1. At the continuum level: extending the formalism of the moving contact line (Blake's or Shikhmurzaev's) to a system that has a time-dependent nonuniform composition

2. At the molecular level: to determine the surface tension of interfaces that have nonequilibrium composition profiles.

3. Develop methods to predict the nonequilibrium tensions from equilibrium tensions as a function of composition.

The ultimate goal will be to provide a strategy for CFD of reactive wetting liquid metals that ideally relies exclusively on equilibrium properties of the metal mixtures, and avoids the use of any MD simulations. The latter, and CF-DFT techniques, will only be needed to generate thermodynamic and/or dynamic data, and secondly to help develop new concepts such as surface tensions of nonequilibrium and evolving interfaces

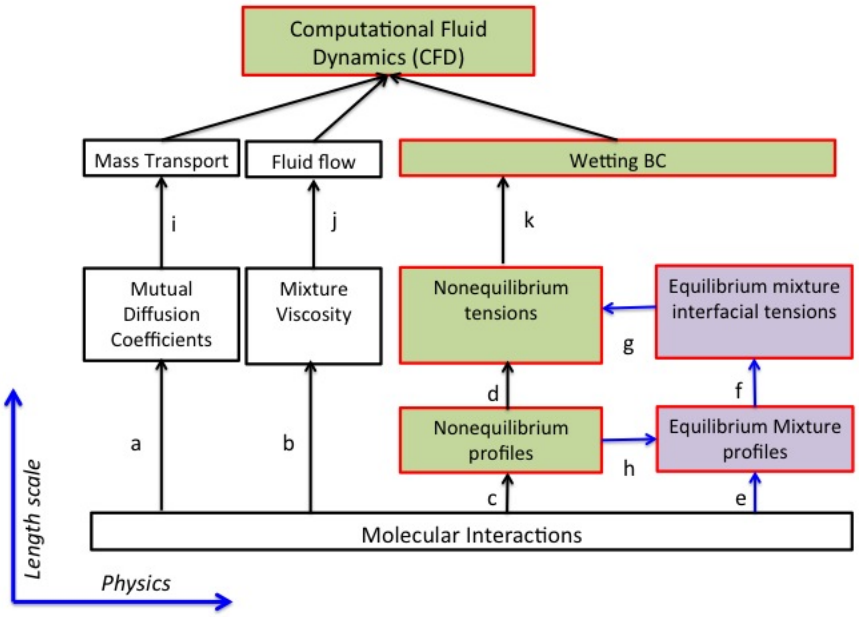

Figure 2.1. Diagram of the proposed predictive computational fluid dynamics (CFD) model for reactive wetting. The CFD requires diffusion parameters (i) for mass transport, and viscosity information (j) to solve the Navier-Stokes equations. The boundary conditions (BC) needed for the contact line movement are one of two approaches, one suggested by Blake the other by Shikhmurzaev. Both require adaptation to nonuniform mixtures and interfacial tension information(k). The mutual diffusion coefficients for metal mixtures can be obtained (a), ultimately, from self-diffusion coefficients that are either generated by molecular dynamics (MD) or molecular kinetic theory (e.g., Enskog approximations). The viscosity can be obtained (b) from MD or molecular theory. The interfacial tensions (k) that feed into the contact angle BCs can be obtained from the noneqilibrium density profiles (c&d). This can be accomplished by MD or classical fluids DFT. Alternatively, the nonequilibrium profiles produce nonequilibrium tensions by developing methods that use equilibrium information. That is indicated by the path (h, f, g). The required equilibrium tensions can be generated by MD or DFT (see path(e,f)). The color scheme for the boxes is as follows. Black indicates that the methods or data are well-established. Green indicates that established simulation of theoretical methods need to be used to generate the information. Red indicates that some level of new science and innovative research is required. The strategy to accomplish that is described in this document.

Diffuse interfaces

In what follows we will consider a surface reaction as representing the interfacial processes of preferential adsorption, surface reaction and dissolution. In this approach it is the liquid phase that undergoes changes (initially inside the interfacial region and potentially beyond during later stages) while the solid phase stays the same. We recognize that dissolution *does* lead to a diffuse interface, where one fluid atom replaces another solid atom as the solid phase dissolves. This produces an interface that is therefore more diffuse (in terms of composition and/or structure) than one would surmise from the fluid side alone. To capture this aspect better, one needs to consider, in detail, whether the assumption of a flat interface can still be considered correct. If that is the case, it would appear that the dissolution can be considered a surface reaction.

The concept of a surface reaction introduces two time scales. One associated with the rate of reaction, the other with the diffusion process. There will be an interplay between these and the timescale that characterizes the movement of the contact line. In addition, the cooling process introduces its one time scale set by the thermal diffusion.

Temperature gradients

During metal joining both temperature variation and significant temperature gradients are likely to occur. The gradients gradually disappear as the liquid phase spreads and cools down as it approaches a final equilibrium. All the materials parameters (including tensions, viscosity and reaction rates) relevant to the spreading problem depend on T. CFD codes can treat the flow of energy coupled with fluid flow, and thus in principle simultaneous heat effects can be included in the computational treatment. To do so faithfully, requires information about the temperature dependence of the surface tension, the viscosity and the diffusion coefficients. As long as the fluid stays in the liquid phase, this does not constitute a serious challenge. However, phase transformations either in the liquid phase, but more commonly during solidification can complicate the overall picture. This is because solidification is a highly nonlinear coupled process.

Solidification

During (or following) the spreading or infitration by the liquid metal, parts of the liquid will reach a condition that is either a glassy state, or a state point beyond a phase boundary, where the current, super-cooled, liquid phase becomes unstable with respect to liquid-phase separation, or unstable with respect to crystallization (or both). A phase transformation heralds an abrupt change of certain materials properties. For instance, crystallization will cause an enormous increase in some properties, i.e., the viscosity (a near divergence), an enormous decrease in others such as the diffusivity. Other properties will undergo step changes (e.g., density, heat capacity).

Crystallization proceeds by nucleation and growth, and depending on 1) how rapidly the cooling takes place, and 2) on the composition as well as the spatial variation of the composition, the

final structure will typically end up displaying many crystalline domains or grains, meeting at grain boundaries.

If the system manages to avoid crystallization then the atom's dynamics will be arrested in a more gradual way. This can be the likely result of compositional effects. Two metals A and B may be miscible in the liquid phase over a large range of composition, but at low temperature the equilibrium crystal may be of a distinct stoichiometric composition, such as AB_2. A liquid sample of initially equal amounts of A and B will need to phase separate as well to grow into a AB_2 crystal. If the mutual difusion coefficients of A and B atoms is sufficiently slow (for a given gooling rate) then the fluid may not be able to nucleate and grow the AB_2 phase. Instead, the result would be a glassy phase of equal amounts of atoms A and atoms B. Alternatively, small crystalline regions of AB_2 may from but end up coexisting with a A-rich glassy phase.

This part of the metal joining process concerns the phase transformation in metal mixtures from the liquid phase. The ultimate kind of microstructure that results is a well-studied area, and previous research has revealed that the microstructure is a strong determinant of the future materials behavior of the metal joint. In conclusion, solidification of the metal joint can, for the purposes of this paper, be considered an essentially understood phenomenon that can be treated with existing strategies.

The important conclusion is that the spatial composition variation of the fluid phase (as it results from the reactive wetting process) serves as the initial state for the solidification. Hence, a sufficient understanding of the wetting process may have an important role to play in determining a desirable final microstructure of the metal joint.

For instance, consider manufacturing a metal joint through an infiltration process as depicted in figure 1.1b. The surface reaction will produce atoms B whose spatial distribution is nonuniform, as different parts of the infltrating liquid have experienced different residence times inside the pore. Near the meniscus we expect to see more uniformity and a higher concentration, whereas near the entrance (on the reservoir side), we expect smaller concentrations of B and less uniformity.

A predictive modeling capability would enable one to explore the *inverse optimization* problem: what initial composition distribution(s) of the infiltrating liquid at the entrance would produce a final joint after infiltration that is most uniform (and thus most desirable)? This could be powerful as it enables fine control over the final properties of a metal joint.

This page intentionally left blank.

Chapter 3

Moving Contact Lines

The moving contact line on a solid surface

Measurements indicate that the value of the contact angle depends on the relative velocity of the solid and liquid. For instance, when a tape is immersed into a liquid at a rate U, it is found that the contact angle at the three-phase contact line (where the solid, liquid and vapor phase meet) increases with U. The measured angle is referred to as a dynamic contact angle, denoted θ_d, to distinguish it from the static contact angle, θ_s. The latter is a material property, and expressed by Young's equation in terms of three surface free energies:

$$cos\theta_s = \frac{\gamma_{sv} - \gamma_{sl}}{\gamma_{lv}} \tag{3.1}$$

It is well-known that the classical hydrodynamic description of flow near a moving contact line runs into problems. The conventional no-slip boundary condition between liquid and solid does not mesh with the concept of a moving contact line, and the stresses near the contact line diverge.

There are essentially two approaches to attempt to fix the problem of a moving contact line. The hydrodynamic theory stipulates that there fluids spread by rolling over the solid, and there is dissipative viscous flow within a wedge of fluid near the contact line. Shikhmurzaev is the main proponent of this view, building on approaches by Dussan and others. The molecular kinetiic approach, due to Blake, on the other hand views flow as a stress-modified rate process that focuses on the immediate molecular environment of the contact line. where attachment and detachment of fluid molecules must occur, causing friction (and thus dissipation).

Blake's approach [9, 10]

Blake has derived the following expression for the wetting-line velocity

$$U = 2\kappa_0\lambda sinh[\gamma_{lv}(cos\theta_s - cos\theta_d)\lambda^2/2kT] \tag{3.2}$$

where κ_0 is the equilibrium frequency of random molecular displacements inside the three-phase zone, and λ is the average distance of the displacements. The product $\kappa_0\lambda$ is thus a velocity. Further, k denotes Boltzmann's constant and T is the absolute temperature. When the argument of the sinh function is small, we can expand around $U = 0$, and obtain a linear form

$$U \approx \kappa_0\lambda^3\gamma_{lv}(cos\theta_s - cos\theta_d)/kT \tag{3.3}$$
$$\equiv \zeta^{-1}\gamma_{lv}(cos\theta_s - cos\theta_d) \tag{3.4}$$

The coefficient $\zeta = kT/\kappa_0\lambda^3$ can be interpreted as a friction coefficient for the wetting-line motion. A later version of Blake's approach further expresses the frequency κ_0 in terms of the work of adhesion (between liquid and solid), i.e.,

$$\kappa_0 \approx \frac{kT}{\eta v_m} e^{-W_a/kT} \tag{3.5}$$

and hence,

$$\zeta \approx \frac{\eta v_m}{\lambda^3} e^{W_a/kT} \tag{3.6}$$

where the η is the bulk liquid viscosity, and v_m is the molecular flow volume. Note $\zeta > \eta$, and increases with stronger interactions between the liquid and solid phase.

The Blake approach to a moving contact angle appears simple, but given that there is no way to predict the three parameters (λ, κ_0 and ζ), it must rely on experimental data to determine the values.

Shikhmurzaev's approach [8, 10]

Analysis of the flow kinematics of experimental observations indicate that a liquid spreading on a solid effectively undergoes a rolling motion. The liquid-vapor interface passes through the wetting line and ends up as part of the liquid-solid interface. That is, a fluid element, initially at the liquid-vapor interface, arrives at the three-phase region, travels through that region in a finite time, and becomes a fluid element at the solid boundary. In this picture, the fluid element has to change its surface properties such as the surface tension from liquid-vapor values to those of the liquid-solid interface. This indicates that there exits a surface tension gradient near the three-phase region, and the values will differ from the equilibrium values. As the contact line moves, a force balance equation still holds at the three-phase point, which we express as the *dynamic* Young's equation:

$$cos\theta_d = \frac{\tilde{\gamma}_{sv} - \tilde{\gamma}_{sl}}{\tilde{\gamma}_{lv}} \tag{3.7}$$

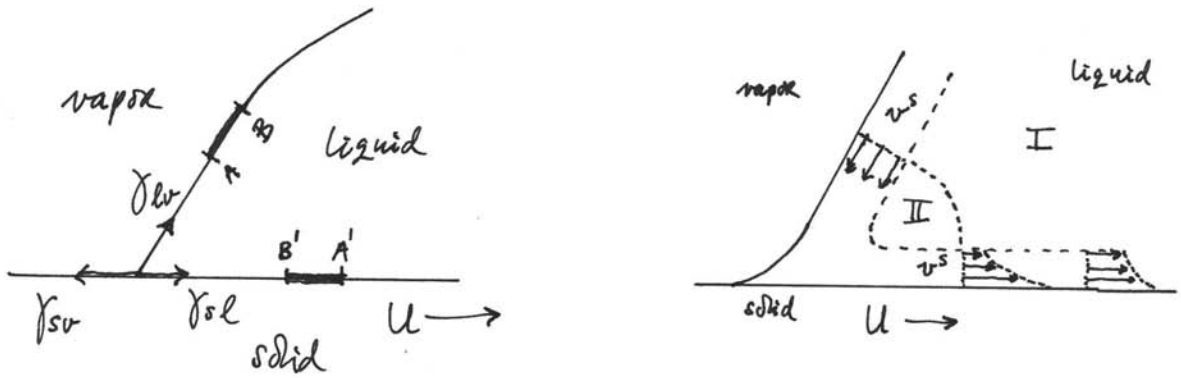

Figure 3.1. Shematic of the contact line. Young's equation is illustrated on the left. On the right hand side we illustrate the flow (ala Shikhmurzaev) in the vicinity of the contact line. The interfaces are depicted as layers of finite thickness so that the velocity distribution across the interface can be depicted. The extent of the contact line region (II) is of the order of Ca (the capillary number). Note that at the solid boundary, and away from the contact line, the magnitude of v^s increases. Slip is present only in the contact region.

where the $\tilde{}$ is used to distinguish the tensions from the equilibrium values of equation 3.1. Given that the surface tensions during movement will be different from the static values we immediately conclude that $\theta_d \neq \theta_s$.

Since the motion of the fluid element (moving from the liquid-vapor interface to the liquid-solid interface) is coupled to the flow field of the entire fluid phase, its relaxation process and thus the values of the $\tilde{\gamma}$'s (and thus θ_d) must depend on the bulk hydrodynamics as well as the flow geometry [1].

Shikhmurzaev's model allows for a nonlocal hydrodynamic influence on contact line movement. He postulates that the surface tension of the ij interface can be expressed in terms of a surface excess density, viz.,

[1]This is an important observation, as it makes clear that formally θ_d can not be expected to be simply some function, f, of the velocity U and a collection of materials parameters, $\chi_1, \chi_2, \ldots$ alone. That is, the assumption that $\theta_d = f(U, \chi_1, \chi_2, \ldots)$ must be incomplete.

$$\gamma_{ij} = c_{ij}(\rho_{ij}^{s,0} - \rho^s), \qquad i = l; \;\; j = v, s \tag{3.8}$$

where $\rho_{ij}^{s,0}$ is a phenomenological constant associated with the interface between phases i and j. The coefficient c_{ij} is an equilibrium property, inversely proportional to the liquid compressibility. Shikhmurzaev considers only the effects on the liquid-vapor and liquid-solid interfaces, assuming that the vapor-solid interface is always at equilibrium, hence, $i = l$, and $j = v, s$.

The continuity equation for ρ^s is,

$$\frac{\partial \rho^s}{\partial t} + \nabla \cdot (\rho^s \mathbf{v}^s) = \frac{\rho^s - \rho_{ij}^{s,eq}}{\tau}; \quad i = l; \;\; j = v, s \tag{3.9}$$

which includes the relaxation of ρ^s toward its equilibrium value, $\rho_{ij}^{s,eq}$.

This equation is combined with an equation that relates the velocity vector, $\mathbf{v}_s$, to the surface tension gradient. For the liquid-vapor and liquid-solid interfaces these are, respectively:

$$(1 + 4\alpha_{lv}\beta_{lv})\nabla\gamma_{lv} = 4\beta_{lv}(\mathbf{v}_s - \mathbf{u}) \tag{3.10}$$

$$\mathbf{v}_s = \frac{1}{2}(\mathbf{u} + \mathbf{U}) + \alpha_{sl}\nabla\gamma_{sl} \tag{3.11}$$

where the constants α_{ij} and β_{ij} characterize the viscous properties of the ij interface.

The distribution of the surface parameters, and thus the $\tilde{\gamma}$'s, are linked through the dynamic Young's equation (equation 3.7). and the condition that the flux of ρ^s into and out of the contact line has to balance, allowing rolling motion:

$$(\rho^s \mathbf{v}^s)_{lv} \cdot \mathbf{e}_{lv} = (\rho^s \mathbf{v}^s)_{sl} \cdot \mathbf{e}_{sl} \tag{3.12}$$

where the unit vectors $\mathbf{e}_{ij}$ are normal to the wetting line and tangential to the ij interface.

The above equations are complemented with the usual conditions linking the normal and tangential stress to curvature (at the liquid-vapor boundary) and Navier condition (at the liquid-solid boundary) to form a closed set.

Moving contact line for reactive wetting

We will now briefly consider the case of reactive wetting. For simplicity and definiteness we will consider a fluid of type A that undergoes a simple isomerization reaction at the surface, turning

some A molecules into B. As the reaction proceeds, B molecules will diffuse away from the solid-liquid boundary into the 'bulk' phase and toward the liquid-vapor interface. As a result of the surface reaction induced composition changes at the solid-liquid boundary, γ_{sl} will directly change with time. Indirectly, as molecules B reach the liquid-vapor interface (by diffusion and/or flow), γ_{lv} will change. If the amount of liquid is finite, say a droplet spreading on a surface, and the reaction sufficiently rapid, all of the liquid will become an equilibrium mixture, and both surface tensions reach their stationary mixture values.

The challenge is then to adapt either Blake's or Shikhmurzaev's approach to a moving contact line while taking into account the surface reaction. For this we need to develop an understanding of how γ_{lv} and γ_{sl} change as the surface reaction proceeds. This requires some new development, as we require the nonequilibrium surface tensions as a function of the *local* (i.e., in the interfacial region) composition profile. Note that this is to be distinguished from the straightforward problem of obtaining (or generating) values for γ_{lv} and γ_{sl} as a function of equilibrium mixture of *bulk* composition $\mathbf{x} = x_A$.

Suppose that the surface reaction's equilibrium constant is such that it runs to completion, converting pure A liquid into pure B liquid. Clearly then, we know the values of γ_{lv} and γ_{sl} at $t = 0$ and the corresponding values at $t = \infty$. Namely, they are the two end points on a γ versus x_A plot. During intermediate times the tensions will presumably follow some 'trajectory' connecting the two endpoints, but it is not obvious how to relate this to the equilibrium plot of γ versus x_A. This is because there is no obvious way to assign a single value to x_A to a non-equilibrium composition profile. The sections below address this particular aspect of the entire reactive wetting problem in more detail, and discuss how molecular simulation and DFT can be used to generate the required understanding, and ultimately generate the values of *gamma* as a function of time.

Thus far, we have considered a simple isomerization surface reaction to explain the basic issues and challenges. More complicated reactions, or more complicated mixtures add complexity, but do not introduce problems that are fundamentally different.

This page intentionally left blank.

Chapter 4

Surface Tensions

Modeling liquid metal mixtures

Figure 2.1 indicates that molecular-level information is required to supply the continuum level code with the necessary input regarding 1) bulk mixture thermodynamics, 2) bulk mixture dynamics (diffusion and viscosity) and 3) nonequilibrium surface tensions as a function of (local) composition. Of these three areas the first two have been addressed at length in a recent SAND report, SAND2013-8155, see reference[49]. There we discussed how molecular theory and molecular simulation can be used to supply the required data for thermodynamics, structure and transport quantities.

The fact that for the problem at hand liquid metals can be considered classical simple liquids helps to make the problem considerably more tractable. That is, liquid metals are atomic fluids, and can be successfully described with with interatomic potentials that are spherically symmetric and short-ranged. The classical potential of choice is the embedded-atom method (EAM) potential, which is a multi-body potential with a contribution that depends on the local density surrounding two interacting atoms i and j. As a result of the pair property for the energy, it is straightforward to perform standard molecular simulations (molecular dynamics or Monte Carlo) for metals; and a definition of a local pressure tensor (the negative of the Cauchy tensor) is free of complications, as is the mechanical route to the surface tension.

In addition, just like the quintessential simple liquids, the noble gases, the liquid structure of metals is dominated by the short-range (repulsive) part of the interatomic potential. Loosely speaking, a liquid metal can be considered to be a collection of repulsive spheres moving around in a more uniform attractive background. As a result, one can successfully apply WCA (Weeks, Chandler and Andersen) perturbation theory, which starts by writing the interatomic potential as the sum of a repulsive and an attractive term. The repulsive term is so short-ranged that it can be represented by a hard sphere potential (with a suitable hard sphere diameter). Hence the liquid structure, as expressed by the radial pair distribution function, $g(r)$, and thus all the equilibrium thermodynamic properties can be calculated from the knowledge of the free energy of the hard sphere fluid and the application of an attractive perturbation. The attractive contribution is calculated as an integral over the reference fluid's $g(r)$. This produces very accurate thermodynamic properties of the dense fluid, typically within $1-2\%$ of the values calculated by the 'exact' molecular simulation approach. In a strict mean field theory a further approximation is made: $g(r) \approx 1$.

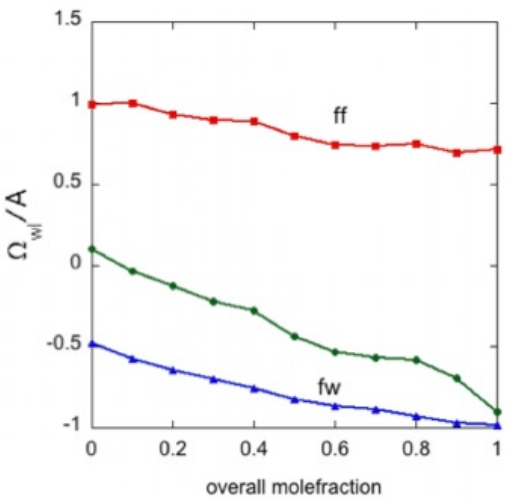

Figure 4.1. The equilibrium surface tension of a solid-liquid interface, Ω_{wl}/A (green curve) for a binary fluid of overall composition x_B.

This, of course, simplifies the calculation at the expense of reduced accuracy of the equation of state.

We refer the reader to that SAND report [49] for further details.

Equilibrium and nonequilibrium surface tensions

Reactive wetting refers to a large class of interfacial phenomena, all of which have in common that the interfacial composition is changing in time. There are several ways in which this may occur. They include dissolution of the solid into the liquid, preferential adsorption of some of the components at the interface, a chemical reaction taking place at the interface. All of these we can consider to some extent as examples of a surface reaction. The key task is then to determine how the presence of the reaction changes the interfacial composition and the interfacial properties (i.e., surface tension).

If the reaction runs till completion the final state of liquid is well-defined and fully defined by its final bulk composition, $\mathbf{x}$ (together of course with the pressure (p), temperature (T)). In that case, we can determine the surface tensions by either MD simulation or CF-DFT, say. Figure 4.1 shows a sketch of the solid-liquid surface tension of some binary liquid metal mixture as a function of composition (here: $\mathbf{x} = x_B$). Now imagine the situation sketched in figure 4.2, which depicts an isomerization surface reaction: $A \to B$. Assume that originally we have a pure fluid at equilibrium at a solid boundary. Starting at time $t = 0$, we allow the surface reaction to take place. Right at the

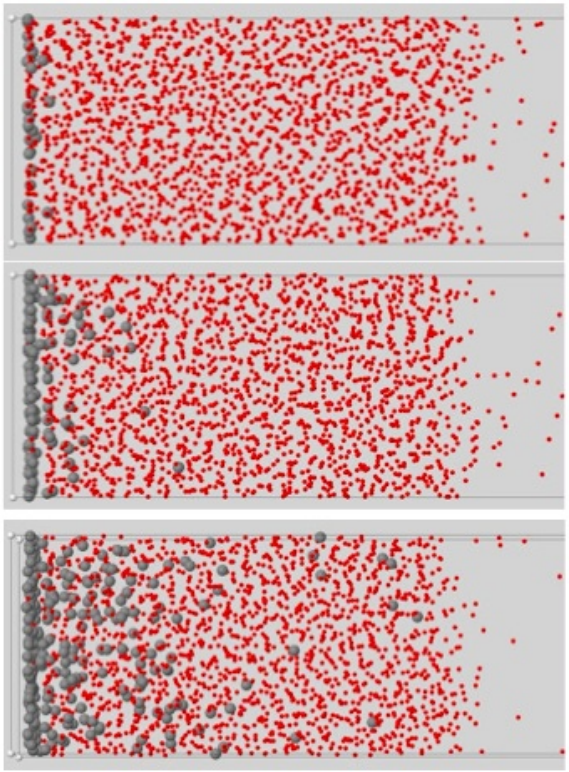

Figure 4.2. A surface reaction-diffusion process. At the left-hand side wall the reaction is $A(red) \rightarrow B(gray)$. To enhance the visibility of species B(gray), the size of atoms A have been reduced. Snapshots taken at different times, progressing from top to bottom. The right-hand side of the box contains a vapor phase. This is a convenient and simple way to represent a *constant* low vapor pressure.

wall, arriving atoms A are converted into B atoms. Thus for $t > 0$ the interfacial composition will start to change. Clearly, for long times, $t \to \infty$, all atoms will have changed into a B, and a new equilibrium fluid has been established.

For such a process, we know the surface tension at the start and at long times. Their values correspond to the end-points of figure, i.e. the tension at $x_A = 1$ and $x_A = 0$. We need to determine the value of γ_{sl} for times in between the two limits.

The composition profile, or more simply, the two profiles as a function of the distance z from the reactive boundary, $\rho_A(z)$ and $\rho_B(z)$, characterize the system. If we assume for simplicity that $\rho_A(z) + \rho_B(z) = \rho =$constant, then only the profile of the product species, B, is required. Several profiles are sketched in figure 4.3 for various times. As time proceeds the contact density $\rho(z = 0)$ or alternatively the molefraction profile $x_B(z)$, increases and so does the extent $\mathscr{L}$ to which species B has diffused into the liquid. Beyond some distance the profile $x_B(z)$ vanishes. At a minimum, this implies that we can not associate any bulk composition x_B with the system. Equilibrium systems are fundamentally different in that an equilibrium profile *would* reach a well-defined bulk value, and hence a surface free energy can be obtained from a tension-composition relationship such as depicted in figure 4.1.

There are, initially, two ways to assign a surface tension to the profiles shown. One is to perform an MD calculation and measure the tension by calculating the integral over the normal and tangential pressure tensor components. The other, more approximate, is to perform a CF-DFT calculation. Both are proceeding on the assumption that the equilibrium expressions for γ apply. In both cases $\gamma_{lv} = \gamma_{lv}[\rho_i(z)]$; $i = A, B$. That is, the surface tension is considered a functional of the entire density profiles of the various components.

A third way could be to map the developing profile at some time t, $\rho_B(z,t)$, onto an *equilibrium* profile $\rho(z, x_A)$ and approximate the tension as $\gamma_{sl}(x_A)$. This would be particularly attractive, as it would reduce the entire nonequilibrium tension effort to generating equilibrium tensions as a function of composition. It seems intuitively clear that such a mapping would require a careful systematic theoretical development. However, an investigation of this kind (by MD or CF-DFT, or a hybrid approach) would appear to be straightforward. An example of such an approach is shown in figure 4.4 where we plot the solid-liquid surface tension, $\gamma_{sl}(t)$. Two cases are shown, that differ in the applied value for the surface reaction probability.

A preliminary simulation study of obtaining nonequilibrium tensions has been performed, and will be discussed elsewhere[51]. In the next section we outline experiments that can be performed to provide experimental information about nonequilibrium surfacee tensions.

Validation experiments

There are two experimental strategies that can provide fundamental information regarding interfacial free energies. One is the feed-through goniometer and the other is measurement of the capillary-driven flow, such as the flow in a V-shaped groove.

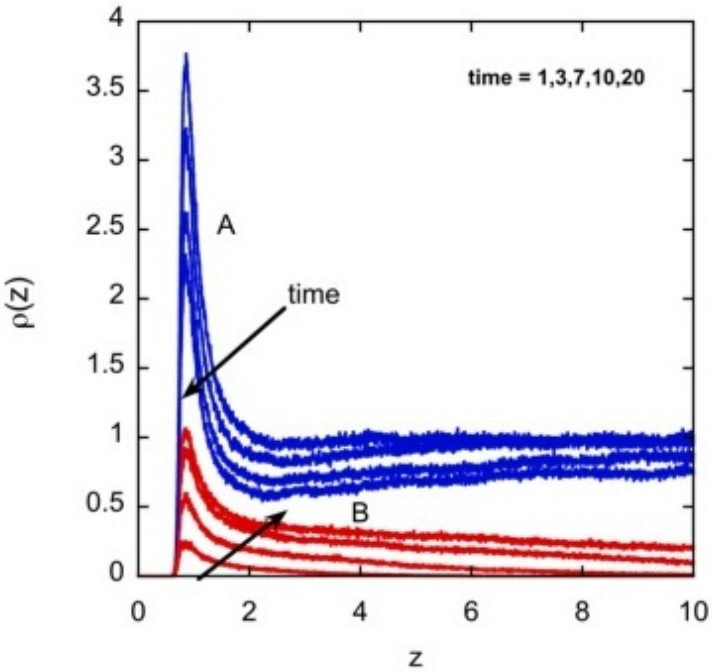

Figure 4.3. A surface reaction-diffusion process. Density profiles $\rho_A(z)$ (blue curves) and $\rho_B(z)$ (red curves) at different times t. Note the transient, non-equilibrium nature of the profiles; all product profiles (i.e., $\rho_B(z)$) approach zero, at larger distances. We can associate a thickness $\mathscr{L}$ with each nonequilibrium profile.

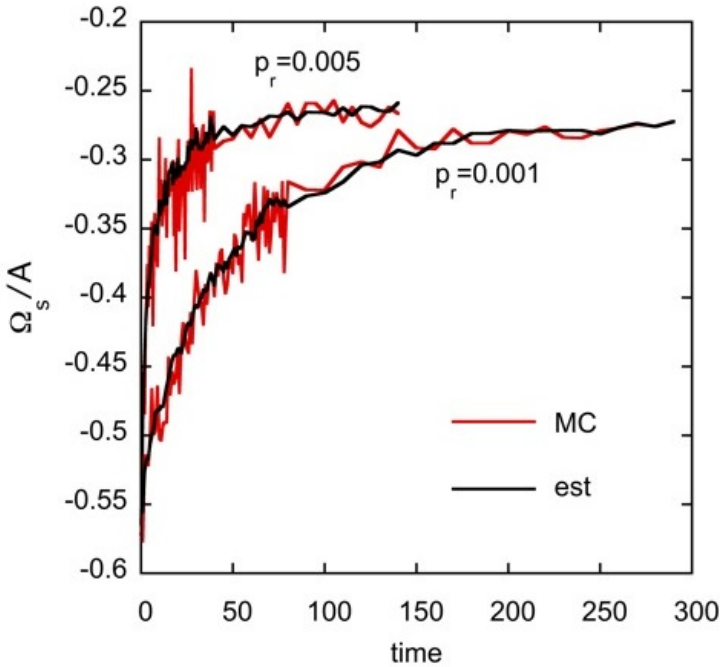

Figure 4.4. A simulation example of the development of the surface tension (here denoted as the surface grand potential per unit area, Ω_s/A) as a function of time, for a surface reaction $A \rightarrow B$. Two cases are shown, differing in the value for the surface reaction probability ($p_r = 0.005$ and $p_r = 0.001$). An estimated surface free energy is shown as a black line. It is based on an integral of the transient profiles shown in figure 4.3.

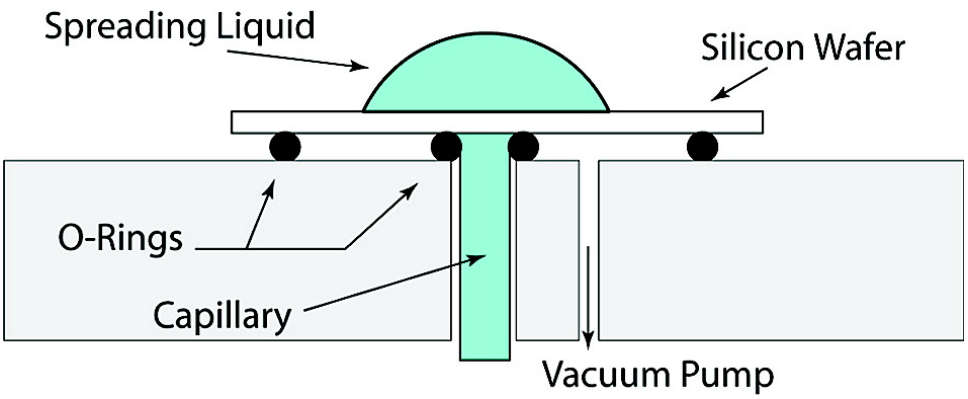

Figure 4.5. Schematic of a feed-through goniometer. This set-up allows the contact-angle measurement of a static sessile drop, or that of a dynamic contact angle at various velocities. see Brooks et al.[30]

The goniometer is illustrated in figure 4.5. Naturally, the challenge for applying the goniometer to studies of most liquid metals is that the temperatures required are high. Brooks, at Sandia, has modified the apparatus in recent years such that it can be now used at high temperatures.

Measurements of capillary flow have a long history that goes back to Lucas and Washburn at the beginning of the twentieth century. Open channel grooves have been first used for liquid metals in the 1940's . Capillary-driven infiltration by a one-component shows that the wetting front position is proportional to the square root of time, $t^{1/2}$, with a constant of proportionality that depends on the contact angle as well as the fluid viscosity.

Both types of experiments lend themselves to study reactive wetting under well-controlled and/or simplifying conditions. Thus, the goniometer can be used to measure static contact angles isothermally at a range of temperatures and for controlled *equilibrium* bulk mixture compositions. Capillary-flow measurements with either the goniometer or the grooves represent nonequilibrium, and non steady-state conditions, but can be performed isothermally and for controlled *equilibrium* bulk mixture compositions, in the absence of reactive/dissolutive interfacial phenomena.

The effects of interfacial reactions can be studied by selecting the appropriate combinations of solid and liquid-metal. The presence of the surface reactions will lead to nonequilibrium interfacial compositions and hence nonequilibrium surface tensions. The initial composition of the liquid-metal remains a parameter to be varied in the experiments, as the effect of the surface reaction on the composition depends on the initial composition.

Whereas the dimensions of the sessile drop (in goniometer experiments) do not affect the dynamic behavior of non-reactive liquid-metals, under conditions of reactive wetting the dynamic behavior is expected to depend on the drop size. That is because the spreading of the products of a surface reaction depends on the drop size. For instance, consider a surface reaction whereby the solid dissolves into the liquid. The time it takes to reach the equilibrium composition depends on

the total volume of the drop[1] , whether there is only diffusion or combined diffusion and convective mass transport. Similarly, the time it takes for the solid atoms to populate the liquid-vapor interface is a function of the drop's height.

[1]Naturally, that time also depends on the drop's shape, i.e., the volume to contact area ratio

Chapter 5

Conclusion

This report describes in detail what research and development is needed to be able to create a continuum-level modeling approach to challenging problems in the area of reactive wetting. A high-fidelity simulation capability for multi-component interfacial dynamics represents a significant advance in the ability to predict wetting, spreading and flow in a number of critical areas of the DOE mission, including manufacturing, flow in porous media, thermal spray and aluminum relocation. With a continuum level tool in place one could, for the first time, readily impact metal joining processes by computationally exploring the effects of varying materials and processing variables such as composition, surface roughness, dimensions, operating times and conditions. It should help reduce the cost of processing and manufacturing, and provide a scientific tool for assessing and controlling product quality.

The strategy outlined here constitutes a good example of multi-physics multi-scale modeling to predict fluid flow under conditions of varying composition (e.g., reactive or dissolutive wetting), using molecular level information that is firmly based in statistical mechanics. The methodology will be applicable to any type fluid (e.g., liquid metals, aqueous solutions), and can be employed in a variety of contexts. The envisioned modeling capability will greatly enhance one's ability to improve the quality of metal joints used throughout the weapons complex. It enables new joining strategies to improve part yield, such as the use of tailored and modulated filler metals. Additionally, the effort is of a general nature (not limited to metals, say) and will impact inkjet printing technologies as well as flow in porous rock.

This page intentionally left blank.

References

[1] J.J. Stephens, F.M. Hosking, C.A. Walker, E.C. Dudley, F.G. Yost *The evolution of a ternary Ag-Cu-Zr active braze filler metal for kovar/alumina braze joints*, Proceedings of the 3rd international brazing and soldering conference, 2006, San Antonio Texas.

[2] E. Moret and N. Eustathopoulos, *Ceramic to metal direct brazing*, Journal De Physique IV Colloque C7, supplement au Journal de Physique 111, Volume 3, novembre 1993

[3] E. A. Carter and E. A Jarvis, *The role of reactive elements in thermal barrier coatings*, Computing in Science & Engineering March-April 2002 pg. 33.

[4] Equilibrium Software HSC Chemistry, see http://www.outotec.com/en/Products–services/HSC-Chemistry/

[5] J-M Zhang, B. Wang and K-W Xu, *Surface segregation of the metal impurity to the (100) surface of fcc metals*, Ind. Acad. Sci. **69**, 603 - 616 (2007)

[6] Y. Rosenfeld, Phys. Rev. Lett., **63**, 980 (1989)

[7] X. Liu, T.J.H. Vlugt and A. Bardow, Ind. Eng. Chem. Res., **50**, 10350 - 10358 (2011)

[8] Y.D. Shikhmurazev, *The moving contact line of a smooth solid surface.*, Int. J. Multiphase Flow., **19**, 589-610 (1993)

[9] T.D. Blake, *Dynamic contact angles and wetting kinetics*, Wettability, Ed. J.C. Berg, Marcel Dekker, New York, 251-309 ,(1993)

[10] T.D. Blake, M. Bracke, and .D. Shikhmurazev *DExperimental evidence of nonlocal hydrodynamic influence on the dynamic contact angle*, Phys. Fluids., **11**, 1995-2007 (1999)

[11] L. Mondy and many others, *Wetting and free surface flow modeling for potting and encapsulation*, Sandia report, SAND2007-3316, Albuquerque, New Mexico,(2007)

[12] P. Protopapas, H.C. Andersen, and N.A.D. Parlee, *Theory of transport in liquid metals. I. Calculation of self-diffusion coefficients.*, J. Chem. Phys., **59**, 15-25 (1973)

[13] P. Protopapas, H.C. Andersen, and N.A.D. Parlee, *Theory of transport in liquid metals. II. Calculation of shear viscosity coefficients.*, Chem. Phys., **8**, 17-26 (1975)

[14] B.J. Alder, D.M. Gass, and T.E. Wainwright, *Studies in Molecular Dynamics. VIII. The Transport Coefficients for a Hard-Sphere Fluid.*, J. Chem. Phys., **59**, 15-25 (1973)

[15] Arrhenius, Z. Physik. Chem., **1**, 285(1887)

[16] L. Grunberg and A.H. Nissan, *Mixture Law for Viscosity*, Nature., **164**, 799-800(1949)

[17] D. Ben-Amotz and D.R. Herschbach, *Estimation of Effective Diameters for Molecular Fluids.*, J. Phys. Chem., **94**, 1038-1047 (1973)

[18] R. Krishna and J.M. van Baten, *The Darken Relation for Multicomponent Diffusion in Liquid Mixtures of Linear Alkanes: An investigation using Molecular Dynamics (MD) Simulations.*, Ind. Eng. Chem. Res., **44**, 6939-6947 (2005)

[19] D. Ben-Amotz and D.R. Herschbach, *Estimation of Effective Diameters for Molecular Fluids.*, J. Phys. Chem., **94**, 1038-1047 (1973)

[20] X. Liu, A Martin-Calvo, E. McGarrity, S.K. Schnell, S. Calero, J-M. Simon, D. Bedeaux, S. Kjelstrup, A. Bardow and T.J.H. Vlugt, *Fick Diffusion Coefficients in Ternary Liquid Systems from Molecular Dynamics Simulations.* Ind. Eng. Chem. Res., **51**, 10247-10258 (2012)

[21] D.R. Wheeler and J. Newman *Molecular Dynamics Simulations of Multicomponent Diffusion 1. Equilibrium Method.*, J. Phys. Chem. B, **108**, 18353-18361 (2004)

[22] D.R. Wheeler and J. Newman *Molecular Dynamics Simulations of Multicomponent Diffusion 2. Nonequilibrium Method.*, J. Phys. Chem. B, **108**, 18362-18367 (2004)

[23] R. Taylor and R. Krishna *Multicomponent mass transfer* 1st ed.; *Wiley*: New York, NY (1993)

[24] D.J. Evans and G.P. Morriss *Statistical Mechanics of Nonequilibrium Liquids*, *Academic Press*: London, UK (1990)

[25] D.K. Enskog, *Svenska Vetenskapsaded. Handl*, 63, 4 (1922)

[26] S. Chapman and T.G. Cowling,*The Mathematical Theory of Nonuniform Gases*, 2nd ed. *Cambridge University Press* (1922)

[27] M.K. Tham and K.E. Gubbins *Kinetic Theory of Multicomponent Dense Fluid Mixtures of Rigid Spheres.*, J. Chem. Phys., **55**, 268-279 (1971)

[28] Lopez de Haro, E.G.D. Cohen and J.M. Kincaid *Kinetic Theory of Multicomponent Dense Fluid Mixtures of Rigid Spheres.*, J. Chem. Phys., **78**, 2746 (1983), and J. Chem. Phys., **79**, 4509 (1983)

[29] J.J. Erpenbeck *Transport coefficients of hard-sphere mixtures: Theory and Monte Carlo molecular dynamics calculations for an isotopic mixture.*, Phys. Rev. A., **39**, 4718-4731 (1989)

[30] C.F. Brooks, A.M. Grillet and J.A. Emerson *Experimental Investigation of Spontaneous Wetting of Polymers and Polymer Blends.*, Langmuir, **22**, 9928-9941 (2006)

[31] B.K. Yen, *X-ray diffraction study of mechanochemical synthesis and formation mechanism of zirconium carbide and zirconium silicides*, Journal of alloys and compounds **268**, 266-269 (1998) .

[32] S. Q. Wang and J. W. Mayer, *Reactions of Zr thin films with SiO_2 substrates*, J. Appl. Phys. **64**, 4711 (1988).

[33] S. Roberts and P.J. Dobson, *Evidence for reaction at the Al-SiO_2 interface*, J. Phys. D: Appl. Phys. **14** L17 (1981).

[34] J.J. Stephens, P.T. Vianco, P.F. Hlava, and C.A. Walker, *Microstructure and performance of Kovar Alumina Joints made with silver-copper active metal braze alloys*, Conference paper SAND99-1577C.

[35] R. E. Loehman and A. P. Tomsia, *Reaction of Ti and Zr with AlN and Al2O3*, Acta metal. mater. Vol. **40**, Suppl., S75 - S83 (1992).

[36] D. H. Kang, I-H Jung, *Critical thermodynamic evaluation and optimization of the AgZr, CuZr and AgCuZr systems and its applications to amorphous CuZrAg alloys*, Intermetallics **18**, 815 - 833 (2010).

[37] R. E. Loehman, B. D. Gauntt, F. M. Hosking, P. G. Kotula, S. Rhodes, J. J. Stephens, *Reaction and bonding of Hf and Zr containing alloys to alumina and silica*, Journal of the European Ceramic Society **23**, 2805 - 2811 (2003).

[38] R. E. Loehman, F. M. Hosking, B. Gauntt, P. G. Kotula, P. Lu, *Reactions of Hf-Ag and Zr-Ag alloys with Al_2O_3 at elevated temperatures*, J. Matls. Sci. **40**, 2319-2324 (2005).

[39] T.C. Shields and J.S. Abell, *Thick films of YBCO on alumina substrates with zirconia barrier layers*, Supercond. Sci. Technol. **5**, 627433 (1992).

[40] A. Christensen and E. A. Carter, *First-principles characterization of a heteroceramic interface: ZrO_2 (001) deposited on an α-Al_2O_3 (1102) substrate*, Physical Review B **62**, 16968 (2000).

[41] R. N. Patil and E.C. Subbarao, *Monoclinic-Tetragonal Phase Transition in Zirconia: Mechanism, Pretransformation and Coexistence*.Acta Cryst. **A26**, 535 (1970) .

[42] T-S Kim, K-H Kim, Takashi Goto and Byong-Taek Lee, *Microstructure Control of Al_2O_3/ZrO_2 Composite by Fibrous Monolithic Process*, Materials Transactions, **45**, No. 2 (2004) pp. 431-434.

[43] V. V. Srdic, S. Rakic, Z. Cvejic, *Aluminum doped zirconia nanopowders: Wet-chemical synthesis and structural analysis by Rietveld refinement*, Materials Research Bulletin **43**, 2727-2735 (2008).

[44] G. Baldinozzi, D. Simeone, D. Gosset, and M. Dutheil, *Neutron Diffraction Study of the Size-Induced Tetragonal to Monoclinic Phase Transition in Zirconia Nanocrystals*, Physical Review Letters **90** 216103-1 (2003)

[45] A. S. Barnard, Rakesh R. Y. and H. Xu, *Modelling the effect of particle shape on the phase stability of ZrO_2 nanoparticles*, Nanotechnology **17**, 3039 (2006)

[46] A. Suresh, M. J. Mayo, W. D. Porter and C. J. Rawn, *Crystallite and Grain-Size-Dependent Phase Transformations in Yttria-Doped Zirconia*, J. Am. Ceram. Soc., **86** 360-62 (2003).

[47] Y. Teraoka, M. Komaki, *Surface segregation and surface melting in segregating alloys*, Surf. Sci. **439** 1-13 (1999).

[48] Y. Teraoka, *A theoretical study of melting*, Surf. Sci., **281**, 317-322 (1993), and *Surface melting and superheating*, Surf. Sci., **294**, 273-283 (1993).

[49] F. B. van Swol, J. E. Miller, J.B. Lechman, and R.E. Givler, *Theory and Modeling of Active Brazing*, SAND Report, SAND2013-8155, (2013).

[50] Landolt-Bernstein New Series IV/5

[51] F. van Swol, to be published.

DISTRIBUTION:

1	MS 0346	Carlton F. Brooks, 1513
1	MS 0836	Richard C. Givler, 1513
1	MS 0836	Jeremy B. Lechman, 1516
1	MS 0836	Scott A. Roberts, 1513
1	MS 0840	Daniel J. Rader, 1513
1	MS 0878	R. Allen Roach, 2735
1	MS 1411	Amy Sun, 1814
1	MS 1411	Frank B. van Swol, 1814
1	MS 0899	Technical Library, 9536 (electronic copy)

This page intentionally left blank.

Sandia National Laboratories